Desalination and Water Treatment
www.deswater.com
1944-3994/1944-3986
doi: 10.1080/19443994.2012.705096

51 (2013) 1344–1351
February

Taylor & Francis
Taylor & Francis Group

A novel solar-driven air gap membrane distillation system

Edward K. Summers, John H. Lienhard V*

Massachusetts Institute of Technology, 77 Massachusetts Ave, Cambridge, MA 02139-4307, USA
Email: lienhard@MIT.EDU

Received 8 April 2012; Accepted 15 June 2012

ABSTRACT

Membrane distillation (MD) is a thermal-based membrane technology that is capable of treating highly concentrated or contaminated brines, including use as part of a zero liquid discharge desalination system. The low temperatures of operation of MD make it ideal to be used with solar energy as a heat source. However, current solar powered MD systems show poor performance and operate at low temperature compared to other thermal desalination systems. This paper describes a novel configuration of air gap MD which employs direct heating of the MD membrane by solar energy. The configuration provides a more uniform temperature profile over the membrane in the flow direction thereby enhancing vapor production. Heat transfer process modeling of the system shows that it can achieve a thermal efficiency that is nearly twice that of current solar powered MD systems.

Keywords: Air gap membrane distillation; Heat and mass transfer; Desalination; GOR; Temperature polarization

1. Introduction

Solar powered desalination has the potential to provide a solution for arid, water scarce regions that also benefit from sunny climates, but which are not connected to municipal water and power distribution networks that are necessary for the implementation of efficient, large-scale desalination systems. Solar energy can provide heat energy or electrical power to a small-scale system that could run independent of any other infrastructure.

The most common form of solar desalination is a solar still. Solar stills are simple to build, but inherently do not recycle energy as water condenses on a surface that rejects heat to the ambient environment [1]. Another option of this type is solar powered reverse osmosis (RO). While being more energy efficient than any thermal-based system, it requires expensive components and is expensive to maintain. The RO membranes experience high pressures and can easily be damaged by substances commonly found in seawater, therefore pretreatment is required. High cost and complexity makes these systems unattractive for off-grid or developing world applications.

Membrane distillation (MD) has several advantages as a means for desalination and water purification. As a thermally driven membrane technology which runs at relatively low pressure, which can withstand high salinity feed streams, and which is potentially more resistant to fouling, MD could be used for desalination where reverse osmosis is not a good option. The use of thermal energy, rather than electrical energy, and the fact that MD membranes can withstand dry out make this technology attractive for

*Corresponding author.

Presented at the International Conference on Desalination for the Environment, Clean Water and Energy, European Desalination Society, 23–26 April 2012, Barcelona, Spain

Table 1
GOR and operating conditions of existing renewable powered MD desalination systems

System	Type	GOR	Operating condition
Banat et al. [4]	AGMD	0.9	Clear sky, 40.11 kWh/day absorbed energy, 7 m^2 memb. area
Fath et al. [5]	AGMD	0.97	Clear sky, T_{top} = 60–70℃, 7 m^2 area, T_{bot} = 40–50℃, 0.14 kg/s low rate, seawater
Guillen-Burrieza et al. [6]	AGMD	0.8	T_{top} = 80℃+, 20.1 L/min (0.33 kg/s) feed flow rate, 5.6 m^2 memb. area, two modules in series, 35,000 ppm feed salinity
Wang et al. [7]	VMD	0.85	

Operating conditions listed.

renewable power applications where input energy and water production would be inherently intermittent and large quantities of electricity (from photovoltaic cells) would be very expensive. The easy scalability gives it advantages over other large thermal systems such as multistage flash and multi effect distillation for small-scale production.

However, renewable powered MD systems which have been built currently have poor energy efficiency. When measured by the gained output ratio (GOR)[1] these systems do not exceed the performance of a simple solar still, which typically has a GOR of 1, as most solar stills do not usually employ energy recovery [2]. Systems with poor energy performance are generally costlier to run, especially if there is a large capital cost associated with solar collection [3]. Table 1 summarizes the energy performance of existing renewable powered MD systems.

Of all the systems above, air gap MD (AGMD) is the simplest. The heat recovery mechanism is integrated into the module and desalination is achieved with a single flow loop. The air gap between the feed and condensate stream limits heat loss. However, current renewable powered systems use large solar collector arrays which can be very expensive, as they contain not only a solar absorbing surface and glass covers, but piping and structure as well. If this could be further integrated, a complete desalination system could be provided as a single piece of equipment with one pump for fluid circulation thereby reducing capital and resultant water cost.

2. Radiatively heated MD

In the novel configuration proposed here, integration of the heat collection and desalination steps is accomplished by using the MD membrane to absorb solar energy. Instead of the fluid stream being heated and sent to the start of the MD module at an elevated temperature, the saline fluid stream is heated directly at the point of evaporation by solar energy absorbed by the MD membrane. Fig. 1 shows the heat and mass flows along the length of membrane.

This configuration has several distinct advantages over traditional MD systems. Firstly, since the fluid is being continuously heated while it distills instead of being heated before being distilled, the temperature across the module remains higher, increasing the vapor pressure and the resultant flux due to higher evaporation potential. Secondly, since the heat of vaporization is being provided directly from the heat source at the liquid–vapor interface, the resistance to heat flow through the boundary layer is substantially reduced; temperature polarization. Lastly, the entire MD process is now integrated in one device and can take advantage of simple methods of solar collection and concentration, such as using a Fresnel mirror array as shown in Fig. 2.

Some aspects of this design have been investigated previously. Use of direct heating on the membrane to eliminate temperature polarization was experimentally tested by Hengl et al. [8]. Heating was delivered using an electrically resistive metallic membrane which would be impractical to use in a large-scale system. Energy efficiency performance was not measured. Chen et al. [9] used uniform solar flux to heat the feed stream by placing a solar absorbing surface above the feed stream. This method still retained the temperature polarization effect, but captured the idea of integrating solar collection and desalination into one unit.

The feature that strongly distinguishes this system from others developed in the past is a solar absorbing membrane that is placed below the water layer. The membrane can be a dyed single sheet that absorbs solar energy near the MD pores, or a composite membrane with a hydrophilic polymer such as polycarbonate or cellulose acetate, layered on top of a standard MD membrane material, like Teflon (PTFE).

[1]GOR is the ratio of the latent heat of evaporation of a unit mass of product water to the amount of energy used by a desalination system to produce that unit mass of product. The higher the GOR, the better the performance.

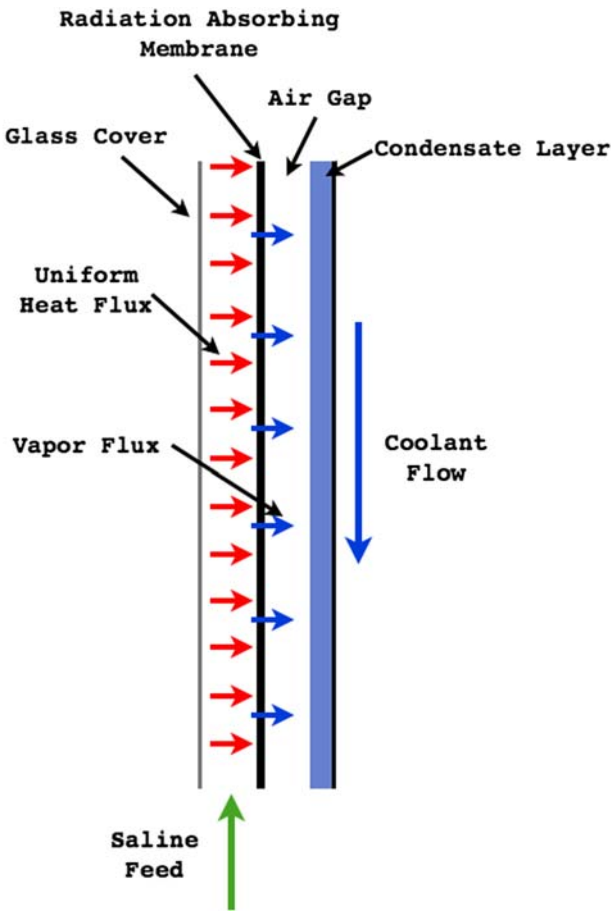

Fig. 1. Schematic diagram of a radiatively heated MD module with energy and mass flows.

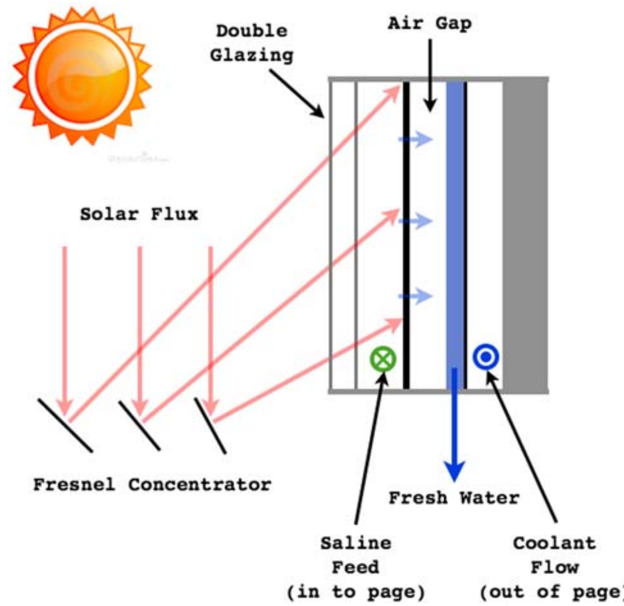

Fig. 2. Side view of a system using Fresnel mirrors to concentrate solar energy.

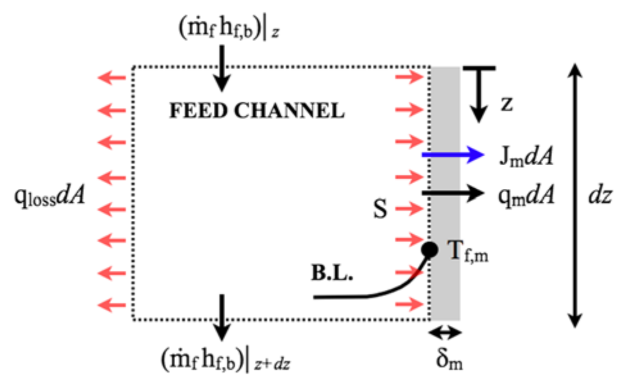

Fig. 3. The hot side of the MD membrane receiving heat flux S, with heat and mass fluxes labeled.

3. Modeling

The MD portion of the system was modeled using equations from Summers et al. [10]. However, in a directly heated system, there is no external heat input and the energy enters at the membrane surface. Since, the surface is exposed to the environment, there are also losses. A control volume of a differential portion of the saline feed channel for this case in shown in Fig. 3.

Without a solar radiation input, the energy and mass balance of the fluid flowing through differential element remain the same as for any other MD system [10]. The solar radiation component enters at the membrane according to Eq. (1):

$$\dot{m}_f dh_{f,b} = -[J_m(h_{fg} + h_{f,m} - h_{f,b}) + q_m]dA + SdA \tag{1}$$

where the subscripts f,b and f,m are the feed, the bulk fluid, and membrane on the feed side. q_m is the conductive heat loss through the membrane, and J_m is the vapor flux. Consolidating and collecting terms, Eq. (2) shows that the solar input, S is distributed among sensible heating of the feed stream; energy to evaporate the liquid; and conductive losses through the membrane, respectively:

$$SdA = \dot{m}_f dh_{f,b} + J_m(h_{fg} + h_{f,m} - h_{f,b})dA + q_m dA \tag{2}$$

The temperature difference between the feed in the bulk stream and at the membrane surface can be found using the heat transfer coefficient $h_{t,f}$ between the bulk and membrane where heat flowing from the membrane to the bulk increases the temperature of the bulk stream over the length of the module as described in Eq. (3):

$$m_f dh_{f,b} = h_{t,f} dA(T_{f,m} - T_{f,b}) \tag{3}$$

3.1. Solar transmission

The quantity S is determined by the transmission characteristics of the cover system. Since fluid flows over the absorber plate, this fluid becomes an additional material in the cover system, attenuating the energy that reaches the absorber.

A system of two covers was described by Duffie and Beckman [1] which would account for incidental reflections between covers; however, a good approximation for most solar collectors is that the transmission through the next cover is a fraction of what is transmitted through the previous cover [1]. This is described by Eq. (4) with the entry angle of the light into the next cover is the exit angle of the previous cover.

$$\tau_2 = (1-\rho_2)(1-\alpha_2)\tau_1 \tag{4}$$

α and ρ are the fractions of energy lost by absorption and reflection, respectively. τ is what is transmitted.

The water layer below the second cover acts as an additional cover. Reflection through the water is a function of the entry angle of a beam of light that exits the glass above it.

$$n_{gl} sin(\theta_{in}) = n_w sin(\theta_{out}) \tag{5}$$

The perpendicular and parallel components of reflection are defined by Eq. (6) and can be used to find the total reflectivity of the water layer in Eq. (7).

$$r_{\parallel} = \frac{\tan^2(\theta_{out}-\theta_{in})}{\tan^2(\theta_{out}+\theta_{in})} \tag{6a}$$

$$r_{\perp} = \frac{\sin^2(\theta_{out}-\theta_{in})}{\sin^2(\theta_{out}+\theta_{in})} \tag{6b}$$

$$(1-\rho_w) = \frac{1}{2}\left(\frac{1-r_{\perp}}{1+r_{\perp}} + \frac{1-r_{\parallel}}{1+r_{\parallel}}\right) \tag{7}$$

where ρ_w is fraction of beam light reflected from the surface of the water, and $r_{\parallel}$ and $r_{\perp}$ are the parallel and perpendicular components of reflectance, respectively. The loss due to absorptivity of the water layer is slightly more complicated. The glass glazings have a relatively constant extinction coefficient in the visible and near infrared where most solar radiation occurs. The extinction coefficient is related to the amount of radiant energy that gets absorbed per unit thickness and is a function of wavelength as described by Eq. (8):

$$\alpha(\lambda) = 1 - \exp\left[\frac{-K_{ext}(\lambda)d}{\cos(\theta_{out})}\right] \tag{8}$$

For water, the extinction coefficient varies in the range of solar radiation wavelengths [11]. Fig. 4 shows the transmissivity of water calculated from the extinction coefficient [11] using Eqs. (7) and (8) compared to borosilicate glass, which is a common glazing material in solar collectors [12].

However, most solar energy that passes through the atmosphere occurs at wavelengths below 1,500 nm. To simplify the model to use one extinction coefficient for the water layer, a power-weighted average is used.

While the extinction coefficient is not related to power linearly, the absorptivity due to the extinction coefficient (Eq. (8)), or the total power attenuated at a specific wavelength, is the absorptivity multiplied by the input power. The power-averaged absorptivity (Eq. (9)) is used directly in the model instead of calculating it from a single extinction coefficient (as can be done for a glass glazing panel using Eq. (8)).

$$\alpha_w = \int_0^{\infty} \alpha(\lambda) I_r(\lambda) d\lambda \bigg/ \int_0^{\infty} I_r(\lambda) d\lambda \tag{9}$$

where I_r is the irradiance in W/m^2 nm. The irradiance can be approximated by using Planck's law of emission from a black body in a vacuum [11], where the sun is approximated as a black body radiating at 5,762 K [1].

$$I_{r,bl}(\lambda) = \frac{2h_p l c_o^2}{n_{air}^2 \lambda^5}\left[\exp\left(\frac{h_{p_l} c_o}{n_{air} k_b \lambda T}\right) - 1\right]^{-1} \tag{10}$$

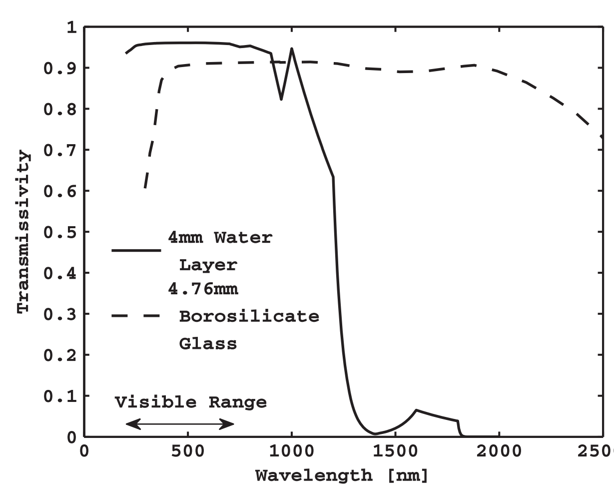

Fig. 4. Transmissivity of solar collector glass compared to water in the visible and near infrared spectrum.

This then allows us to find the total transmissivity of the water layer. Using Eq. (4) the transmissivity of the full stack can be obtained and combined with the solar absorptivity of the membrane to obtain the transmission–absorption product. While the transmission–absorption product is a function of the reflectivity of absorber, the vast majority of opaque absorber materials are minimally reflective and obey the rule described in Eq. (11) [1].

$$(\tau\alpha) = 1.01\tau_{\text{stack}}\alpha_{\text{a}} \tag{11}$$

3.2. Heat loss from top of the module

As with any solar collector, the heated surface is exposed to the environment in order to collect solar energy. This results in a certain heat loss along the length. The heat loss through a cover system has been described in detail [1] as well as in previous work by the authors [13].

The loss through the top is a combination of heat transfer from the feedwater through the cover system and to the environment. Heat transfer modes are shown in Fig. 5.

The loss model further approximates the glass covers as opaque to thermal radiation from low temperature sources, and all energy received from radiation is absorbed and re-radiated at the temperature of the cover. Since the thermal radiation from the top cover sees the sky, it is lost to a sky temperature of 4˚C, and the convective loss is to an ambient air temperature of 25˚C. These conditions are typical of a desert environment on a clear day [14]. Typically, sky temperature is relatively unimportant for calculating collector performance [1]. However, this may become important as the module can run near 90˚C and the radiative loss becomes a higher percentage to the total loss to the environment. Convective loss is determined by known correlations for forced convection over a flat plate [15] and an ambient wind speed of 4 m/s. To minimize loss to ambient air, the characteristic length of flow over the collector can be kept small by spacers that break up the wind along the length.

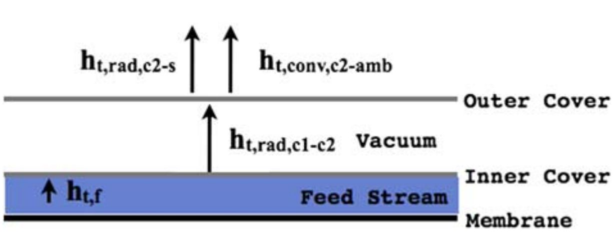

Fig. 5. Loss modes through the solar collecting surface of the module.

4. Cycle configurations and energy efficiency

A uniformly solar heated MD system can be used in different cycle configurations. The simplest configuration is the module itself, which accepts cool saline water at the coolant inlet, and produces fresh water and brine reject at an elevated temperature. Fig. 6 shows this configuration.

Energy efficiency was tested by modeling the complete cycle. Lessons on optimal module designs from previous work [10] were applied to the baseline design for modeling the current system. Table 2 shows baseline operating conditions.

Under these conditions, pressure drop in the flow direction is between 3.5 and 4 atm. For comparison, the liquid entry pressure of a moderately hydrophobic membrane with a contact angle of 120˚ and a pore diameter of 200 nm is around 6.6 atm, allowing the membrane to withstand such hydraulic pressures even if it contains pores that are larger than the mean pore diameter.

The measure of energy efficiency for this device will be the GOR. It is the ratio of the amount of heat needed to evaporate the product water to the actual heat input for the cycle. As this device relies on solar energy, the GOR can be calculated in two ways: The heat input can be taken to be the incident solar radiation, thereby accounting for all the losses in the solar collection step, which for systems that use external

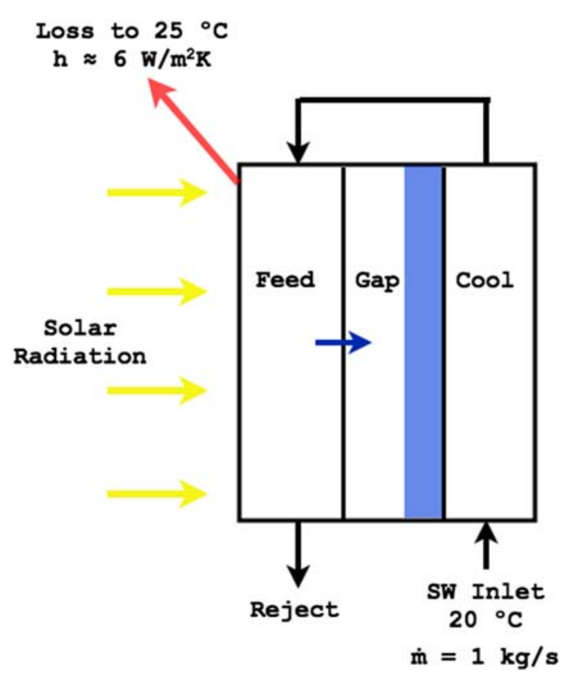

Fig. 6. A basic desalination cycle using the AGMD module.

Table 2
Baseline properties of solar heated AGMD module

Module geometry		*Membrane*	
Effective length, L	145 m	Membrane distillation coefficient, B	16×10^{-7} kg/s m^2 Pa
Width, w	0.7 m	Porosity	0.8
Channel depth, d_{ch}	4 mm	Thickness	200 μm
Air gap, δ_{gap}	1 mm	Conductivity	1.2 W/m K
Operational parameters		*Solar collection*	
Mass flow, $\dot{m}_f, \dot{m}_c$	1 kg/s	Irradiation, I	850 W/m^2
Seawater temperature, $T_{SW,in}$	20°C	Concentration ratio	1
		Glazing separation	30 mm
		Glazing thickness	1.5 mm
		Glazing emissivity	0.8
		$(\tau\alpha)$ Product	0.65

solar collectors is captured by the collector efficiency. The heat input can be taken to be the energy provided to the fluid, which excludes the collection inefficiency and heat loss from the device. Both versions of GOR can be defined in terms of the problem parameters in Eq. (12):

$$\mathrm{GOR}_1 = \frac{\dot{m}_p h_{fg}}{IA} \tag{12a}$$

$$\mathrm{GOR}_2 = \frac{\dot{m}_p h_{fg}}{(S - \bar{q}_{loss})A} \tag{12b}$$

One sun represents 850 W/m^2, the daily mean radiation for summer in a desert climate. The system was modeled at a variety of percentages at that amount. When the heat input was taken to be the incident solar irradiation, GOR for this system was on the order of 1, which is in line with existing solar desalination technologies. When the heat input was taken to be the heat absorbed by the fluid, the GOR can approach three, which is competitive with commercial MD systems [16]. In this cycle, the feed side membrane temperature varies a great deal and goes quite low, as the coolant inlet is fixed at the cold seawater temperature. As a result, the potential for evaporation is reduced and high concentration ratios are required to achieve good performance as shown in Fig. 9. If the temperature of the membrane was higher and more even over the length, the potential for evaporation would be higher and performance improves for the same solar heat input. This is accomplished by using a recovery heat exchanger, as shown in Fig. 7.

The temperature over the module length is not necessarily more flat, but higher overall, as shown in Fig. 8. Most of the heat recovery in the system is done in the heat exchanger. This however, comes at the cost of additional losses, as the hotter feed fluid is exposed to the environment.

Fig. 9 shows how the energy efficiency of this system varies with heat input. Overall, the system with regeneration performs better for a given amount of energy input, especially when the heat input to the fluid is used as a basis for GOR (GOR_2). This has the distinct advantage of eliminating the need for concentrating collectors and performing better during low

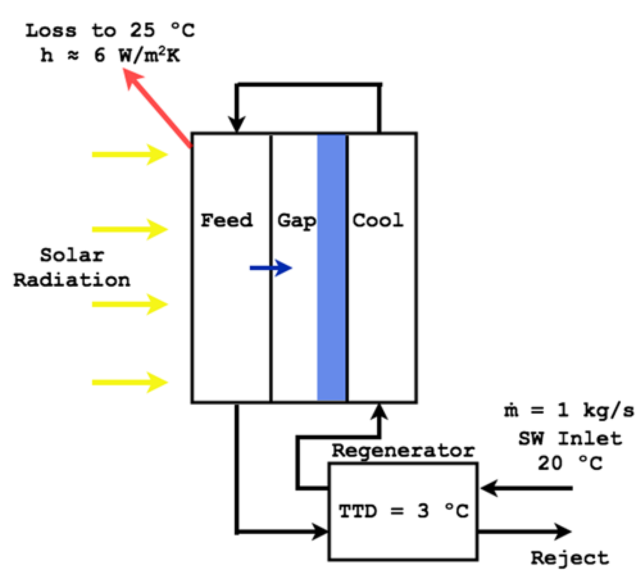

Fig. 7. The AGMD desalination unit with recovery heat exchanger at the bottom of the cycle.

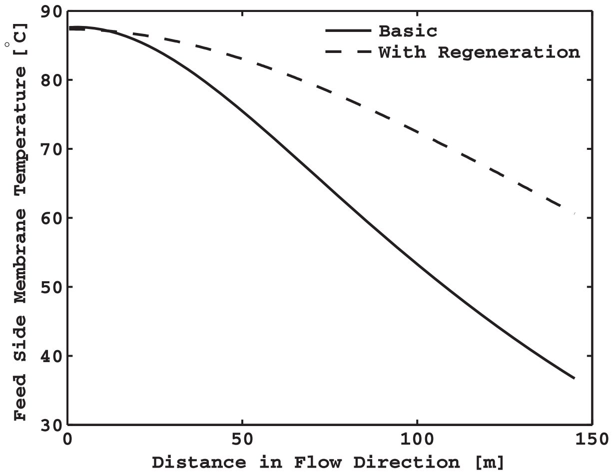

Fig. 8. Temperature profile of the feed side of the membrane along the collector length with and without recovery at an insolation of one sun.

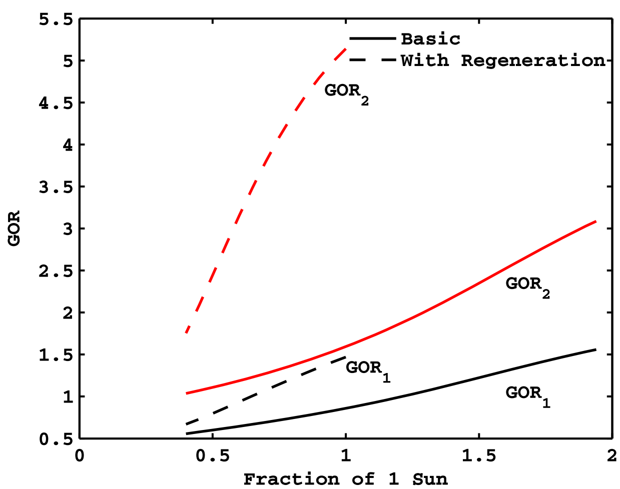

Fig. 9. GOR as a function of degree of solar concentration with and without regeneration.

solar insolation periods, such as dawn and dusk. Since losses make up a greater fraction of the heat input, and are not linearly related to temperature, the difference between the two definitions of GOR becomes more apparent. For the highest insolation at one sun, this corresponds to a 28% efficient solar collector.

5. Conclusions

A novel MD system using direct radiant heating of the membrane has been described. This device is promising in improving solar powered desalination in a simple, effective single or two-piece device. It has the advantages of integrating solar collection into a single device, and delivering heat directly to the source of evaporation, reducing temperature polarization, and increasing vapor flux. A simple liquid–liquid heat exchanger can be added to improve performance, allowing the device to function well during low insolation periods. This device has the potential to achieve performance that exceeds both that of existing solar stills and that of more complex solar powered MD systems.

Acknowledgments

This work was funded by the Cooperative Agreement between the Masdar Institute of Science and Technology (Masdar Institute), Abu Dhabi, UAE and the Massachuetts Institute of Technology (MIT), Cambridge, MA, USA, Reference No. 196F/002/707/102f/70/9374.

Symbols

A — surface area, m^2
c_0 — speed of light, m/s
dA — differential area, m^2
dz — differential module length, m
h — specific enthalpy, J/kg
h_{fg} — latent heat of vaporization, J/kg
h_{pl} — Planck's constant, J s
h_t — heat transfer coefficient, W/m^2 K
I — irradiation, W/m^2
I_r — irradiance, W/m^2 nm
J_m — vapor flux through the membrane, kg/m^2 s
k_b — Boltzmann's constant, J/K
K_{ext} — glazing extinction coefficient, 1/m
$\dot{m}$ — mass flow rate, kg/s
n — index of refraction
$\bar{q}$ — loss average heat loss across the device, W/m^2
q_m — heat flux through the membrane, W/m^2 K
r — reflectance
S — solar radiation flux absorbed by the membrane, W/m^2
U_t — overall heat loss coefficient, W/m^2 K

Greek symbols

$(\tau\alpha)$ — transmission–absorption product
λ — wavelength, nm
α — absorptivity
ρ — reflectivity
θ — beam angle, rad
τ — transmissivity

Subscripts

$\parallel$ — beam component parallel to surface
$\perp$ — beam component perpendicular to surface
a — absorber

air	—	air
b	—	bulk flow
bl	—	blackbody
c1	—	inner cover
c2	—	outer cover
conv	—	convective heat transfer
f	—	feed
gl	—	glazing material
in	—	in
m	—	membrane
out	—	out
rad	—	radiative heat transfer
stack	—	glazing stack

References

[1] J.A. Duffie, W.A. Beckman, Solar Engineering of Thermal Processes, Wiley, Hoboken, NJ, 2006.
[2] S. Parekh, M.M. Farid, J.R. Selman, S. Al-hallaj, Solar desalination with a humidification–dehumidification technique—a comprehensive technical review, Desalination 160 (2004) 167–186.
[3] R.B. Saffarini, E.K. Summers, H.A. Arafat, J.H. Lienhard V, Economic evaluation of stand-alone solar powered membrane distillation systems, Desalination 299 (2012) 55–62.
[4] F. Banat, N. Jwaied, M. Rommel, J. Koschikowski, M. Wieghaus, Desalination by a "compact SMADES" autonomous solar-powered membrane distillation unit, Desalination 217 (2007) 29–37.
[5] H.E. Fath, S.M. Elsherbiny, A.A. Hassan, M. Rommel, M. Wieghaus, J. Koschikowski, M. Vatansever, PV and thermally driven small-scale, stand-alone solar desalination systems with very low maintenance needs, Desalination 225 (2008) 58–69.
[6] E. Guillen-Burrieza, J. Blanco, G. Zaragoza, D.-C. Alarcon, P. Palenzuela, M. Ibarra, W. Gernjak, Experimental analysis of an air gap membrane distillation solar desalination pilot system, Journal of Membrane Science 379 (2011) 386–396.
[7] X. Wang, L. Zhang, H. Yang, H. Chen, Feasibility research of potable water production via solar-heated hollow fiber membrane distillation system, Desalination 247 (2009) 403–411.
[8] N. Hengl, A. Mourgues, M. Belleville, D. Paolucci-Jeanjean, J. Sanchez, Membrane contactor with hydrophobic metallic membranes: 2. Study of operating parameters in membrane evaporation, Journal of Membrane Science 355 (2010) 126–132.
[9] T.-C. Chen, C.-D. Ho, Immediate assisted solar direct contact membrane distillation in saline water desalination, Journal of Membrane Science 358 (2010) 122–130.
[10] E.K. Summers, H.A. Arafat, J.H. Lienhard V, Energy efficiency comparison of single-stage membrane distillation (MD) desalination cycles in different configurations, Desalination 290 (2012) 54–66.
[11] J.R. Howell, R. Siegel, M.P. Menguc, Thermal Radiation Heat Transfer, fifth ed., CRC Press, New York, NY, 2011.
[12] Y. Touloukian, Y. Ho (Eds.), Thermophysical Properties of Matter, vol. 8, Thermal Radiative Properties: Nonmetallic Solids, Plenum Press, New York, NY, 1972.
[13] E.K. Summers, S.M. Zubair, J.H. Lienhard V, Air-heating solar collectors for humidication–dehumidication desalination systems, J. Solar Energy Eng. 133 (2011) 011016-1–011016-6.
[14] W. Underground, Weather History for Dhahran, Saudi Arabia, Online, 2011.
[15] J.H. Lienhard, V.J.H. Lienhard IV, A Heat Transfer Textbook, 3rd ed., Phlogiston Press, Cambridge, MA, 2006.
[16] G. Lange, G. van Gendt, F. Bollen, W. Heinzl, K. Zhao, T.G. Fane, Demonstrating solar-driven membrane distillation using Memsys vacuum-multi-effect-membrane distillation, in: Proceedings of the IDA World Congress on Desalination and Water Reuse, Perth, Australia, September 5–9, 2011, International Desalination Association, Topsfield, MA, 2011.